Compression strength of a fibre composite main spar in a wind turbine blade

Jensen, Find Mølholt

Publication date:
2003

Document Version
Publisher's PDF, also known as Version of record

Risø-R-1393(EN)

Compression Strength of a Fibre Composite Main Spar in a Wind Turbine Blade

Find Mølholt Jensen

Risø National Laboratory, Roskilde
June 2003

Abstract

In this report the strength of a wind turbine blade is found and compared with a full-scale test, made in the same project. Especially the postbuckling behaviour of the compression flange is studied. Different compressive failure mechanisms are discussed and the limitations in using the Finite Element Method. A suggestion to the further work is made.

.

ISBN 87-550-3184-6
ISBN 87-550-3185-4 (Internet)
ISSN 0106-2840

Print: Pitney Bowes Management Services Denmark A/S, 2003

Preface

This report describes part of the work that was carried out in the project "Fundamentals for improved design of large wind turbine blade of fibre composites, based on studies of scale effects. “Phase 1" supported by the Danish Ministry of Environment and Energy through an EFP-fund (journal no. 1363/01-01-0007). The project ran from March 2001 to December 2003 as collaboration between Risø National Laboratory (Project leader), Department of Mechanical Engineering, The Technical University of Denmark, Department of Mechanical Engineering, Aalborg University, Vestas Wind System A/S and LM Glasfiber A/S.

Originally, the project was planned as a 3-year project. But following the wish of the Danish Energy Agency, a 1½-year ("Phase 1") project was formulated

Contents

1 Introduction

The report introduces the complexity of geometrical nonlinear analysis simulating fibre composite in compression. In this project the Finite Element Method (FEM) is used to solve the geometrical nonlinear analysis.

The focus has been on the FEM-problems of simulating large wind turbine blades with load carrying main spars (box girders), but other blade designs may also have the same challengers when they make geometrical nonlinear analysis with fibre composite in compression.

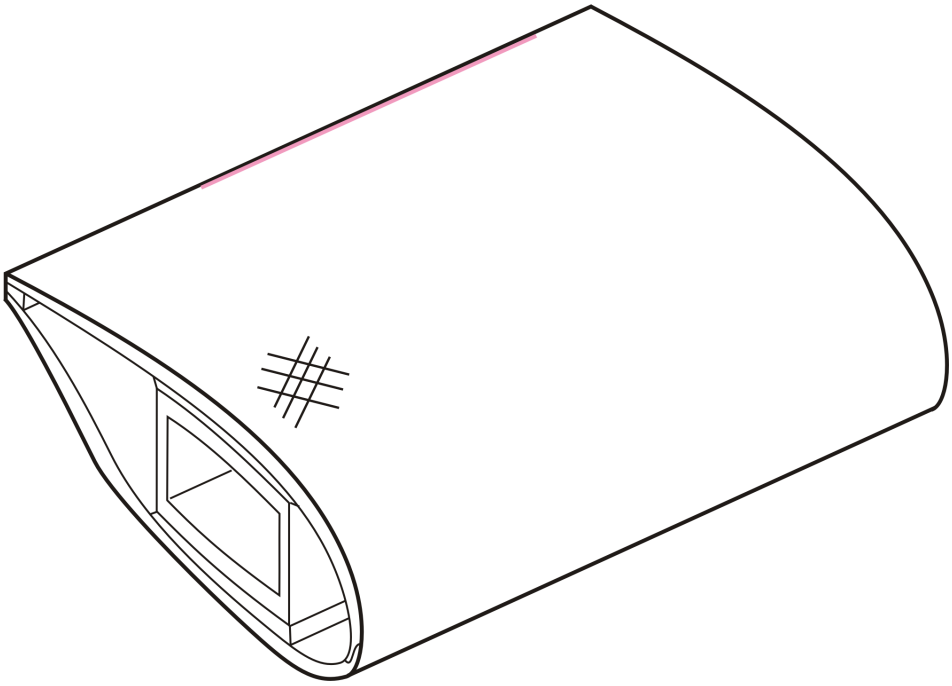

Figure 1. Principle Sketch of Vestas Blade with Main Spar

A FEM-model of the main spar is analysed and results are compared with some results from the full-scale test. See reference 3. Extension and improvements of the FEM-model for further work in the second part are discussed.

The main goal in the work reported here has been to get an overview of relevant failure mechanism and buckling modes for a wind turbine blade, loaded flap-wise.

Different failure modes, imperfection sensitivity, are discussed but not included in the FEM-model. The interlaminar failure mode (delamination) is found to be the most important failure mechanism, and a litterature survey is included in the report to find the state of the art concerning failure mechanisms.

To understand and describe the structural behaviour of the main spar loaded flap-wise, plates and shells with compression load are studied. Based on the post buckling theory and results from the FEM-model and measurement from the full-scale test, an understanding of the structural behaviour of the main spar

is obtained. Especially the structural behaviour of the compression flange is evaluated and compared with the full-scale test.

Furthermore, experiences from the FEM-simulations of the full-scale test with different commercial software and FEM-simulation of wind turbine blade, in the future, are discussed.

2 FEM-simulation of the Full-scale Test

2.1 FEM-Software

Different commercial solvers (Ansys version 6.0, Cosmos version 2.0, MSC-Nastran version 2001r3 and MSC-Marc version 2001) were tested to find advantages/disadvantages for the actual analyses. We have found MSC-Marc-solver best for the actual problem, since it was the easiest solver to reach converge and to find the nonlinear responses path, using Riks method. See next chapter. Furthermore, MSC-Marc has the facility to include material degradation, which is important for the future work.

MSC-Patran Laminate modular version 2001r3 is used as pre- and postprocessor. MSC-Patran Laminate modular is among the best pre- and postprocessor available on the commercial market and it is a big advantage that pre- and postprocessor and solver come from the same software distributor. The FEM-model, only simulating the main spar, is rather coarse and does not include the changes in the geometry near the wing root, ply drops etc, so on this stage a standard pre- and postprocessor would have been sufficient.

2.2 FEM-model Approach

The FEM-model only includes the main spar, since it is the overall structural part, especially when we are looking at the flapwise loads, which is the case for the full-scale testing. See Reference 3+5.

The main spar in a 25 m Vestas blade consists of two symmetrical flanges and two symmetrical vertical webs. The lay-up in the flanges consists of mainly unidirectional fibres orientated in the longitudinal direction. The webs are made of sandwich panels with biaxial fibres in the faces. The flanges have a small curvature (κ) at approximately $\kappa = 1/R = 1/1100\ m^{-1}$, at a position 10 m from the root end.

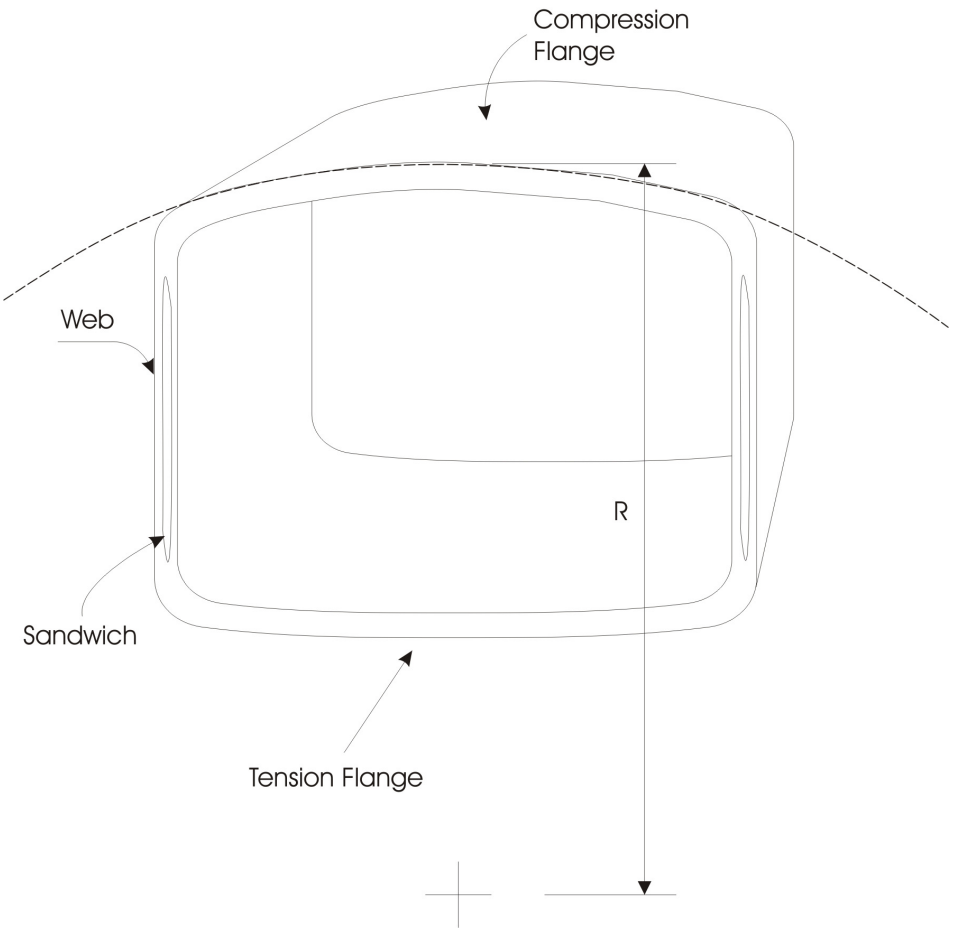

Figure 2. Transverse section of the Main spar

Originally it was the full-scale test 2 (see reference 3+5) which was FEM-modeled, but because of a non-successful collapse in the full-scale (test 2) it was necessary to redefine the FEM-model to represent test 3. The geometry does not include the changes in the geometry near the wing root etc, but will be improved in the future work (phase 2).

The main purpose with the FEM-simulation has not been to make a detailed analysis of the main spar, but to find different failure modes, which could give an input to equip a full-scale test. Inspired from the model results, new buckling detectors were developed to verify the local downward deformation of the compression flange. See full-scale reference 3+5. Furthermore the positions of supports, strain gauges, cameras, and acoustic emissions are improved by the FEM-simulation of the main spar.

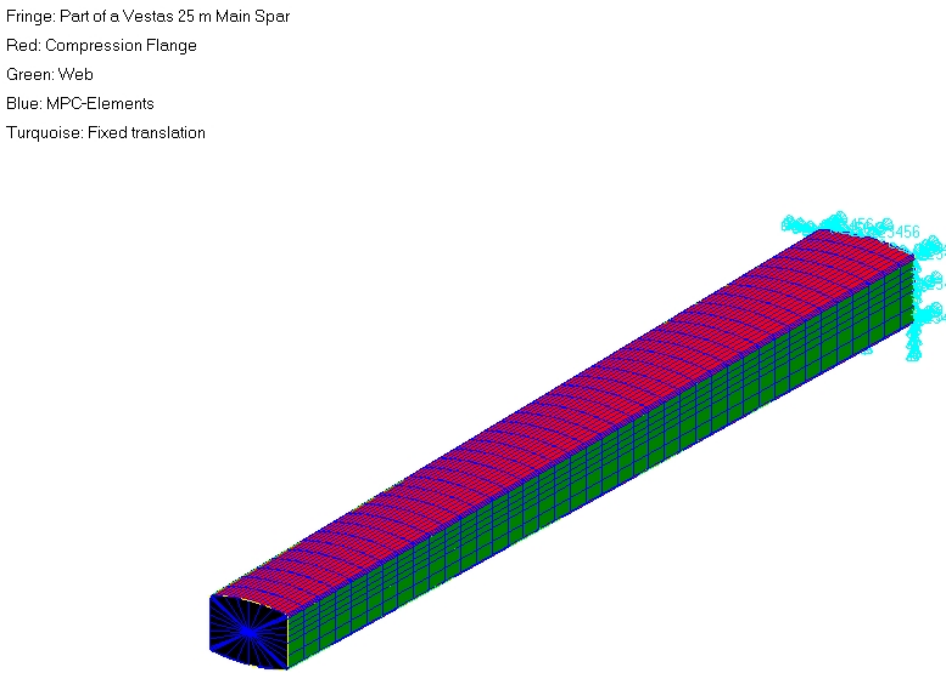

Figure 3. MPC- Elements and Boundaries

2.2.1 Boundaries

All nodes at z=0 are fixed for all translations and rotations. The loads are represented by a single force simulating the full-scale test 3. The single force distributes the loads to the flanges and webs by using MPC-elements. See figure 4 and explanation in the following.

2.2.2 Elements

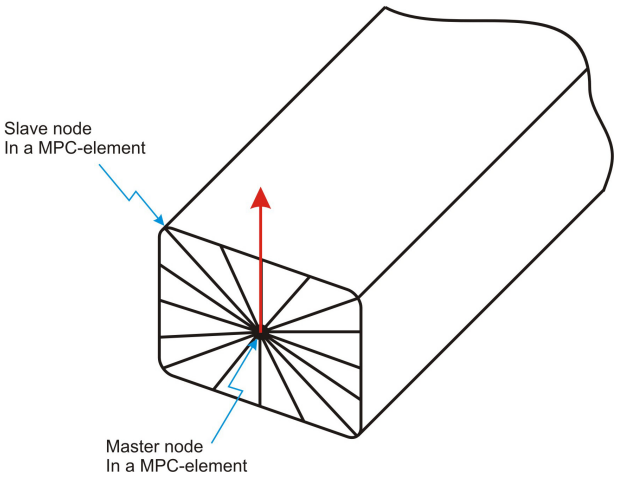

Figure 4. MPC-Element in MSC-Patran/MSC-Marc.

MPC (Multi Point Constrains)-elements are displayed as a set of lines which connect each dependent node (node appearing as part of a dependent term) to each independent node (node appearing as part of an independent term). In this manner, all the nodes are prescribed to have the same displacement in the y-direction. The dependent nodes are circled to distinguish them from the independent nodes. See figure 4.

The main spar is represented by composite shell elements which include orthotropy for each layer, based on Classic Laminate Theory (CLT). The shell element has 4 nodes each with 6 degrees of freedom, 3 displacements and 3 rotations.

The shell element includes out-of-plane shear flexibility, which cannot be neglected for the actual case. For thick plates, shear deformation effects decrease the stiffness which, in turn, decrease the buckling loads. In reference 6 these effects are found to be more significant for laminated composites than for homogeneous, isotropic plates.

The theory used in FEM-simulation only takes into account the shear effect using a first-order shear approximation theory, which can introduce some uncertainty, depending on the shape of buckling mode, orientation of fibre etc.

2.2.3 Composite Lay-up and Material Data

The material data used in the FEM-model, is given by Vestas, and implemented in the FEM-model. The data are not attached to this report, since it is confidential.

The flange lay up consists of a number layers, with mainly unidirectional glass fibre/epoxy laminas.

The webs are made of sandwich and consist of a number of biaxial layers where the layer in the middle is a 5 mm core.

2.2.4 Analysis Type and Load Steps

We assume that all materials possess a linear elastic behaviour; material degradation (kinking, crushing of matrix and fibre) has not been taken into account in the present model.

In the MSC-Marc solver, the geometrical nonlinear response of a structure can be solved by using total or updated Lagrangian formulation. For shell and beam structures one should use updated Lagrangian formulation. See reference 7. When solving for equilibrium, several methods are available for the arc length method. For example the modified Riks nonlinear incremental algorithm, which can be used to construct the equilibrium solution path.

The Riks method are well suited for solving postbuckling analysis. For very stiff structures, one might need to introduce geometric imperfections to get a softer and more realistic structure. For composite plates and shells this can be done by superimposing a small fraction of the lowest eigenmode to the structure. See reference 8. The shape of the fraction is determined by performing a linearized buckling analysis. When superimposing those eigenmodes to the structure one has to re-scale them to a realistic magnitude.

Sometimes it might be necessary to include more than one eigenmode. See reference 8. How many modes one has to include, a convergence test can tell. In the present study, only the lowest eigenmode is used.

Alternatively to model bifurcation from the prebuckling path to the postbuckling path, geometric imperfections of composite plates and shells are introduced by superimposing a small imperfection of the shell thickness.

The analyses are divided into two load cases, both with a unit load of 10 kN. The first load case uses fixed load increments and the second load case find the maximum load increments for each step within for the residual tolerances at 10^5.

2.3 FEM-results

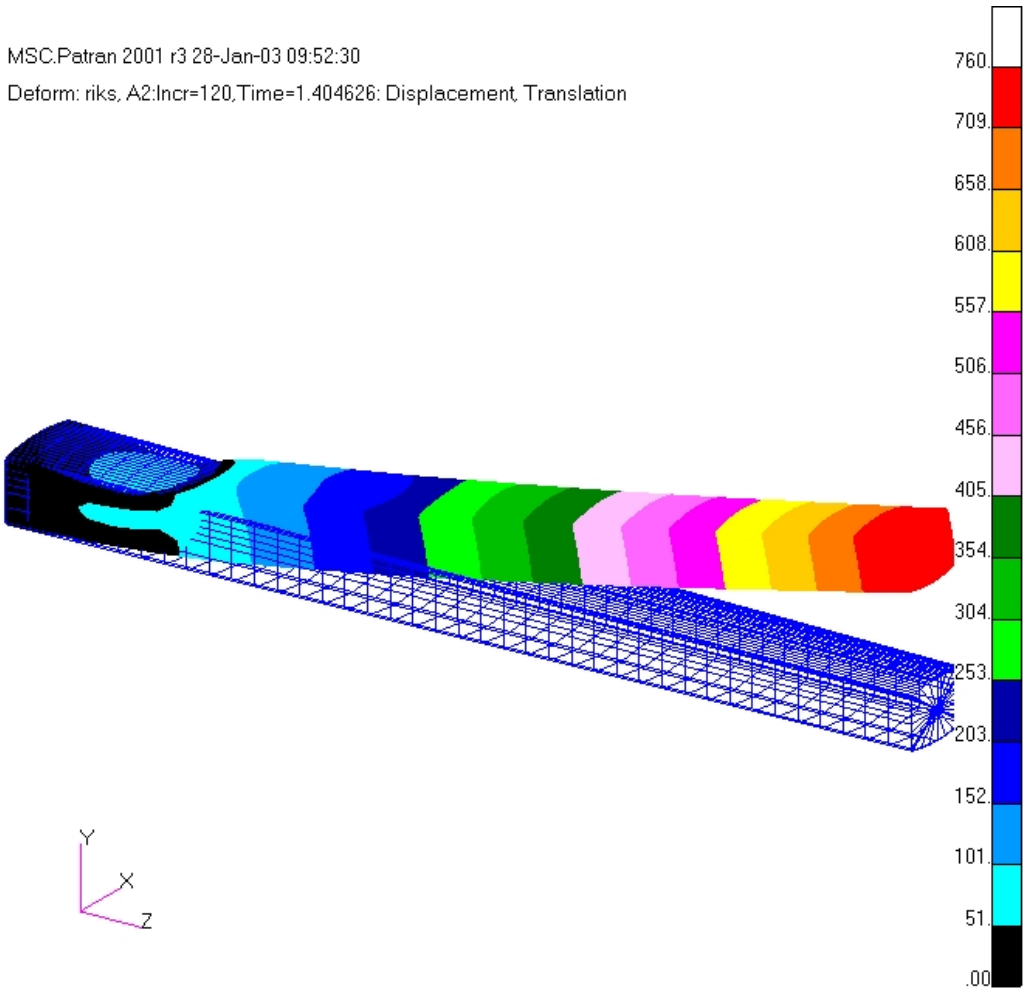

Figure 5. Deformation plot of the Main Spar. The color range is in mm.

2.3.1 Load-Displacement Response of the Main Spar

A deformation plot of the main spar i.e., the relationship between the applied load and the displacement in the load direction (y-direction) is shown in the load-displacement graph. See figure 6. Exhibits linear behaviour (pre-buckling) up to 105 kN where the bifurcation point is reached and a geometrical nonlinear response goes up to 181 kN and the "snap through point" is reached. This snap through load is characterized with having less load-carrying capacity after the limit is reached.

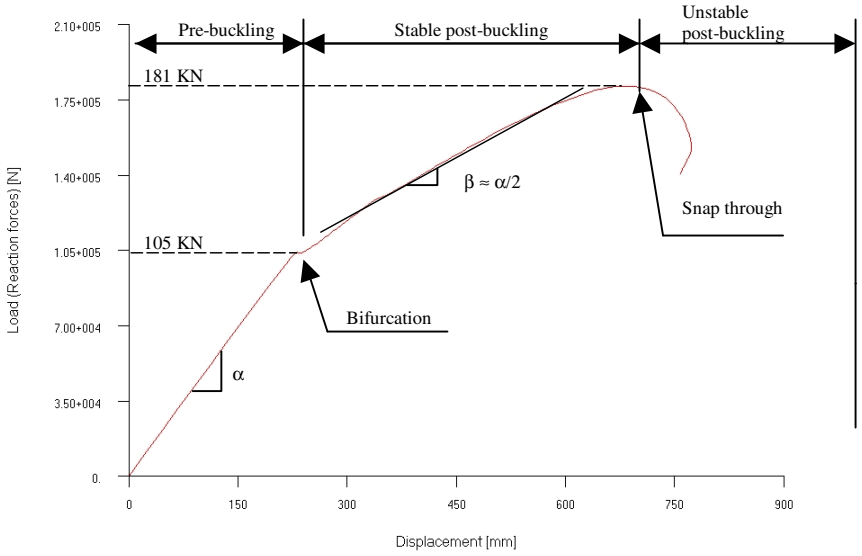

Figure 6. Load-displacement graph of the main spar from FEM-simulation

The load-displacement path exhibits stable postbuckling behaviour after the bifurcation point is reached, and the stable postbuckling phase stops at the snap-through load of 181 kN.

Following the postbuckling path, the compression flange will find a new stable behaviour with approximate half the stiffness. See figure 6. This postbuckling behaviour is characteristic for isotrope plates which are simply supported. See reference 10.

Theoretically the main spar can carry approximately 75 % extra load of the bifurcation load (see figure 6), but in the full scale test the main spar collapse right after the bifurcation load was reached.

The bifurcation point position is confirmed in chapter 5, where local deflection of the flange is evaluated.

2.3.2 Buckling Behaviour (Displacement in the post buckled Section)

The deformation plot shows a relatively large local downward deformation of the compression flange, in point A on figure 7.

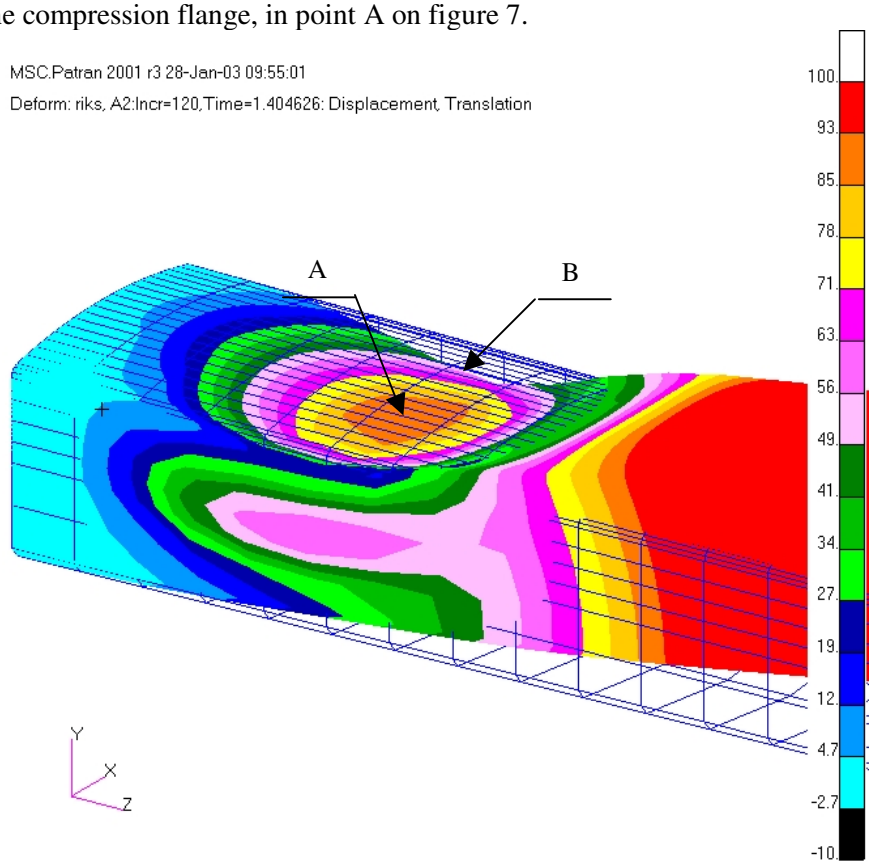

Figure 7. Displacement plot of postbuckled section. The color range is in mm.

When the load reaches a certain level, the deflection of the flange, will "snap through". See the three deformation stages on figure 8.

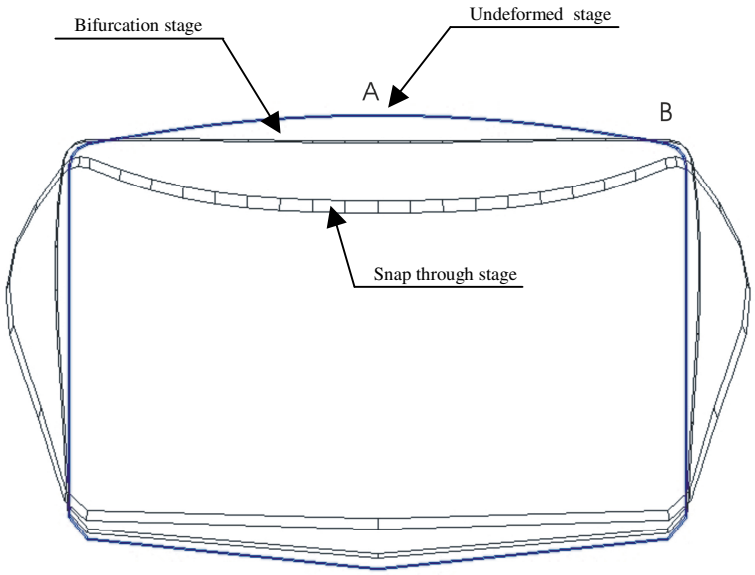

Figure 8. Transverse section of the main spar. Three deformation stages are shown.

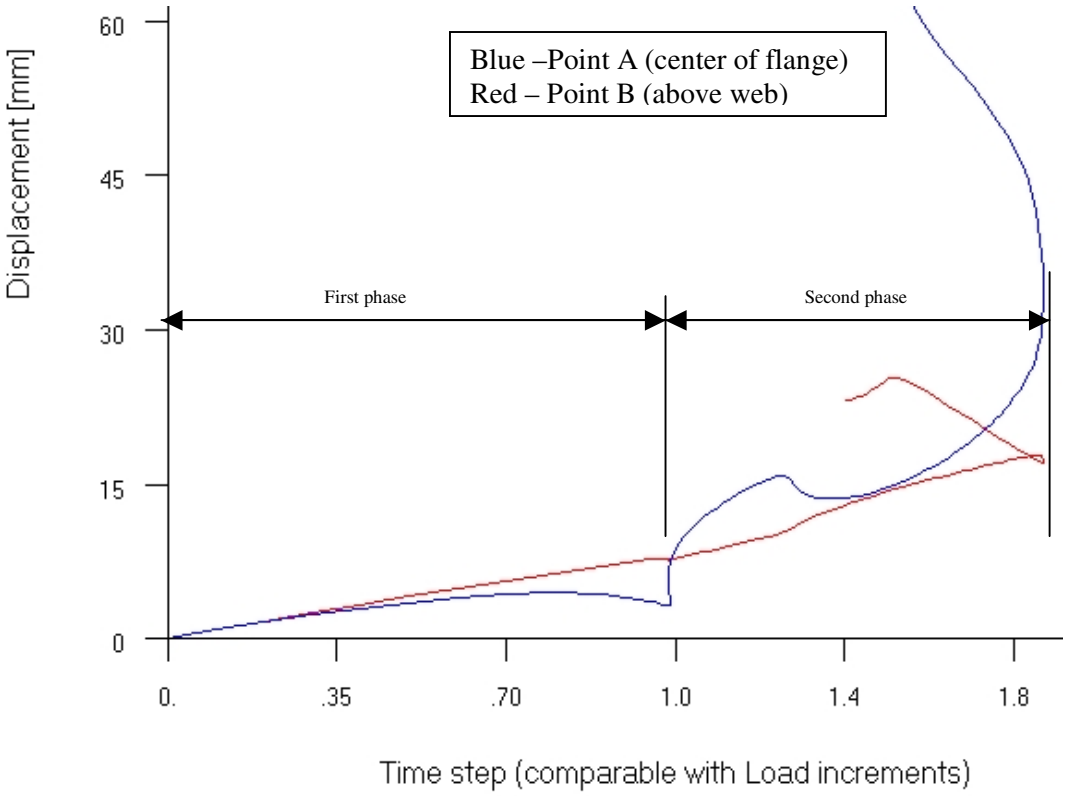

Figure 9. Displacement-Time (load) Graphs for point A and B

The displacements (in the y-direction) versus time are shown on figure 9.

Time can in a Riks analysis be compared with the reaction force (Y-axis), since the time step and the reaction force step are comparable. The reason why time is postprocessed, instead of reaction force, is that the reaction force in a node, which is not subjected to any boundaries, always will become zero as a consequent of the equilibrium criteria.

This assumption is verified. See comparison between figure 6 and figure 10.

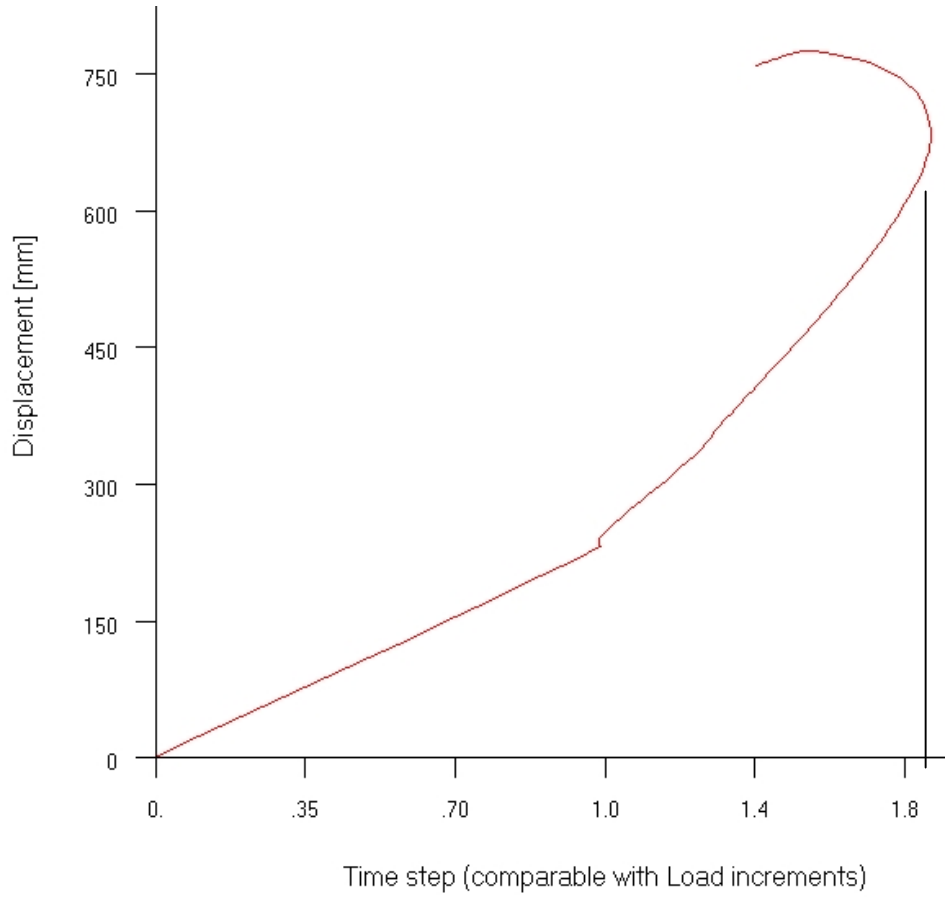

Figure 10. Displacement-Time (load) Graphs for MPC-node (global main spar)

The response in Figure 10 has exactly the same behaviour as the response figure 6. Just the axes have changed order and load steps are replaced with time steps, so the statement "Time can be compared with load-response in a Riks analysis" is verified. The factor between time and load is 10^5.

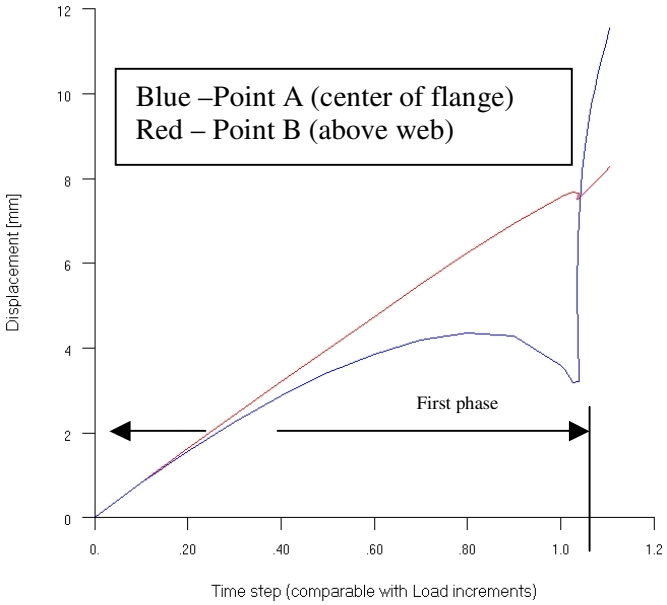

Figure 11. Displacement-Time (load) Graphs for point A and B – First phase

On figure 12, the displacements of point B is subtracted from the displacements of point A, so we compare the same relatively local deformation as can be measured with buckling detectors in a full-scale test. See reference 3+5. Especially the first phase (up to time step 1.0, see figure 9 and 11) is interesting; since we have the same buckling behaviour in the full-scale test. See comparison in chapter 5.

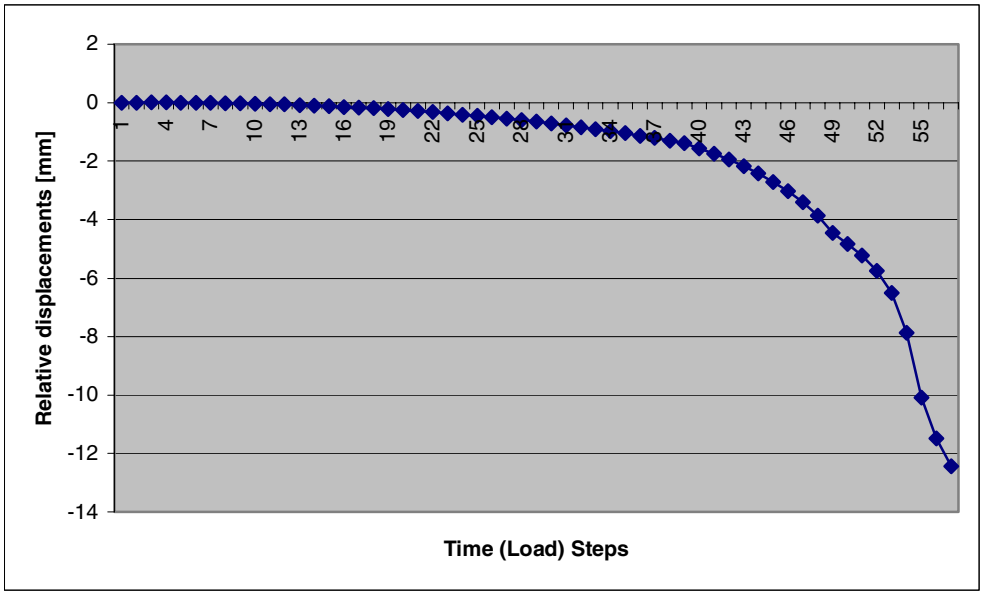

Figure 12. Relative Displacement-Time (load) Graphs – y-displacement of point A minus point B

The explanation to the second phase on figure 9, is much more complex, and further investigation must be made to have the full understanding of the behaviour. For point B (corner node) the relationship between time (load) and displacement is almost linear up to the snap-through point, which also was the case for the main spar in the full- scale test. See comparison in chapter 5.

2.3.3 Strain Evaluation

This part is only very briefly commented, but further investigation in this area could maybe show high stress areas in the structure, which maybe should be reinforced to get a larger caring capacity of the main spar.

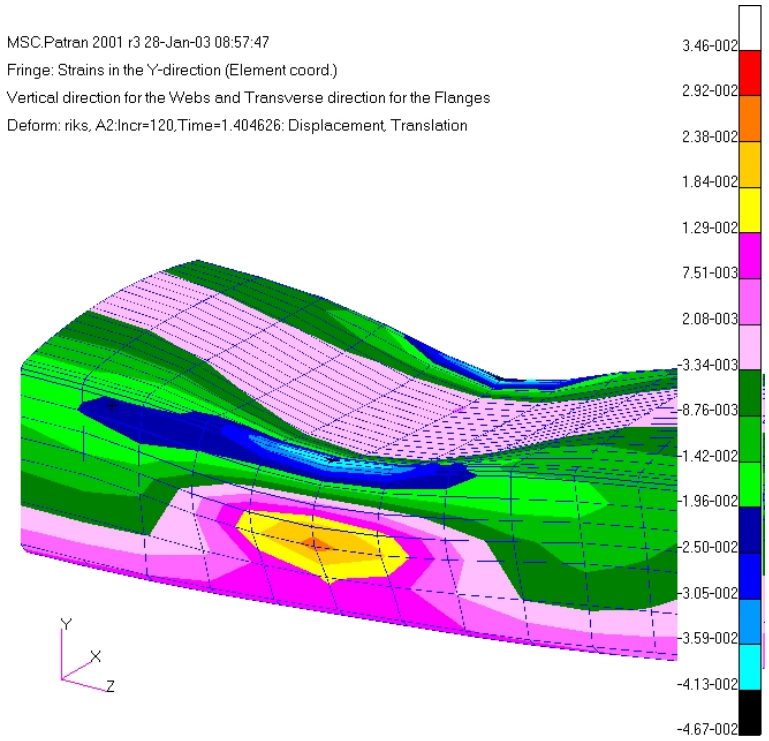

Figure 13. Strains in the main spar. For the flange the transverse (x-direction) strains are shown. For the webs the vertical (y-direction) strains are shown.

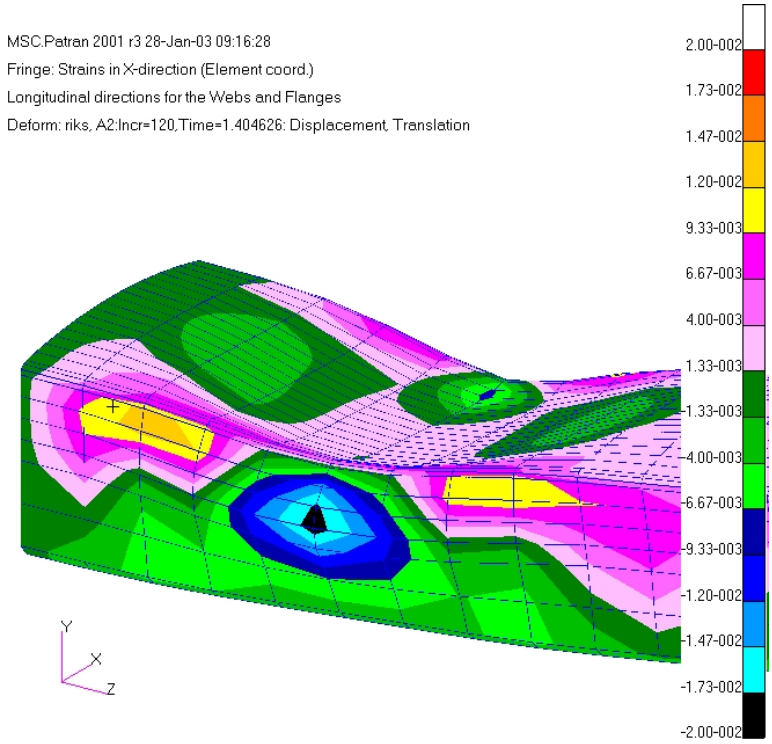

Figure 14. Strains in the longitudinal directions.

3 Theory/References: Linear Bifurcation Buckling and Postbuckling for Composites

To decide whether the main spar exhibits unstable postbuckling behaviour, the geometry of the compression flange must be studied.

When a plate starts to buckle it is usually capable of carrying loads in excess of the linear bifurcation load without collapsing. The reverse tendency is known for curved shells, which do not normally have a stable postbuckling behaviour after the bifurcation load is reached. See reference 9+10.

The FEM-simulation of the load-displacement path (figure 5), of the main spar, has shown a stable postbuckling behaviour after the bifurcation point, which is characteristic for thin isotrope plates. For isotrope cylinder shells the characteristic is normally a non-stable behaviour, so it looks like the main spar acts more like a plane plate than a curved shell. This conclusion is only valid for a main spar without imperfections and delaminations as assumed in the FEM-simulations. In cases where delaminations happen there will not be a long stable postbuckling behaviour and the load capacity will be sensitive for imperfections. See reference 11, 12 and 13.

For imperfection sensitive structures with unstable initial postbuckling paths, the actual buckling strength can be significantly reduced from that predicted by a linear analysis. See reference 17+18. Although the same amount of data does not exist in the case of imperfect laminated shells, it still has been carried out to understand the buckling and postbuckling behaviour of laminated shells.

Zhang and Matthews (reference 13) studied the postbuckling behaviour of cylindrical curved panels of generally layered composite materials with imperfections. Sheinman and Simitses (reference 14), studied the imperfection sensitivity of cylindrical shells under axial compression.

Material and geometric imperfections are not included in the FEM-model, so the load response in figure 6, is only actual for an ideal main spar, which never will be the case in a real main spar design. In the litterature, see for example reference 9+10, constructions with a stable postbuckling behaviour are not so sensitive to imperfections, as structures which have an unstable postbuckling behaviour.

4 Litterature Survey and Discussion: Failure Modes for Composites in Compression

When a plate or a shell is compressive loaded the plate/shell can fail by compressive failure rupture or by loss of in-plane stability. The compressive failure mechanisms on micro scale (kinking, crushing of matrix and fibers etc.) are described in reference 2 and in references 15 and 16. In this report, only brief descriptions of the macro failure mechanisms, which could be relevant for FEM-simulations, are discussed.

The flapwise load is mainly carried by the flanges, as compression and tension, and the webs carry the shear loads. Due to different load conditions and designs, there are several different failure modes for webs and flanges.

4.1 Failure Modes for a Vestas Main Spar - Webs

The reason why webs are made as a sandwich panel is that the rotational stiffness of the corner increases when the bending stiffness of the webs increase. This rotational restraint will introduce tension and compression in the sandwich faces, which can cause wrinkling in the compression faces. See reference 17 and figure 15.

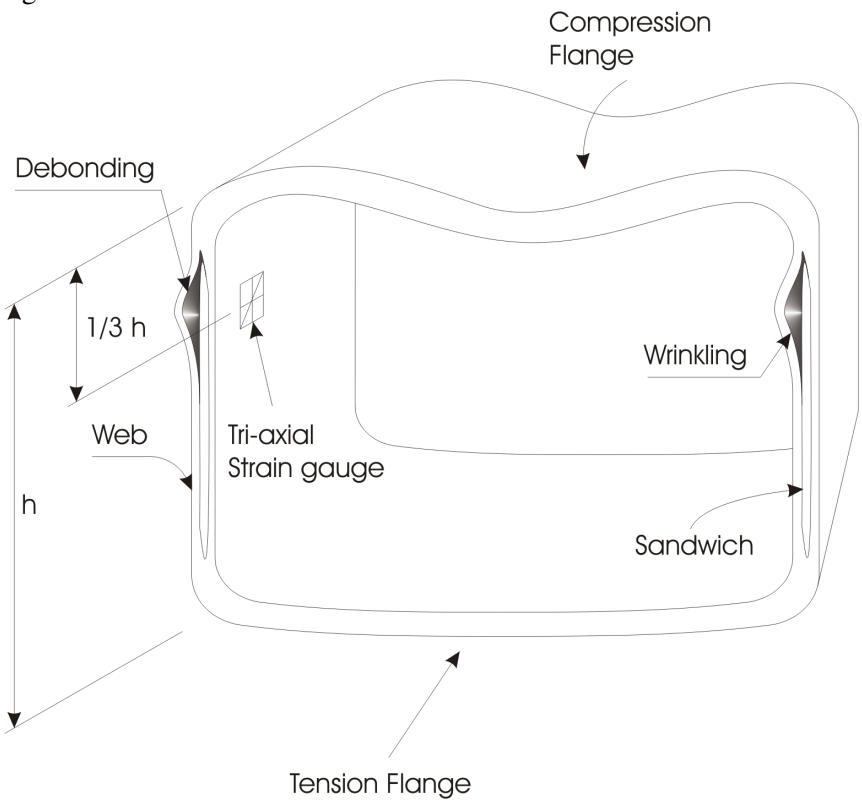

Figure 15. wrinkling including triaksial strain gauges.

In the area - see figure above - there is a complex biaxial stress distribution and the strength and the stability of the faces (wrinkling) must be checked. In the full-scale test a triaxial strain gauge (rosette) was mounted at the inner faces 1/3 h from the top. See figure 10. The measured strain is analysed in reference 3+5.

4.2 Failure Modes for a Vestas Main Spar - Compression Flange

The large downward deformation of point A, see figure 10, may effect in a permanent damage, since the large rotation of the flange introduces high interlaminar stresses between the layers. When the interlaminar stresses are high enough it can effect in delaminations. See figure 16.

4.2.1 Delamination

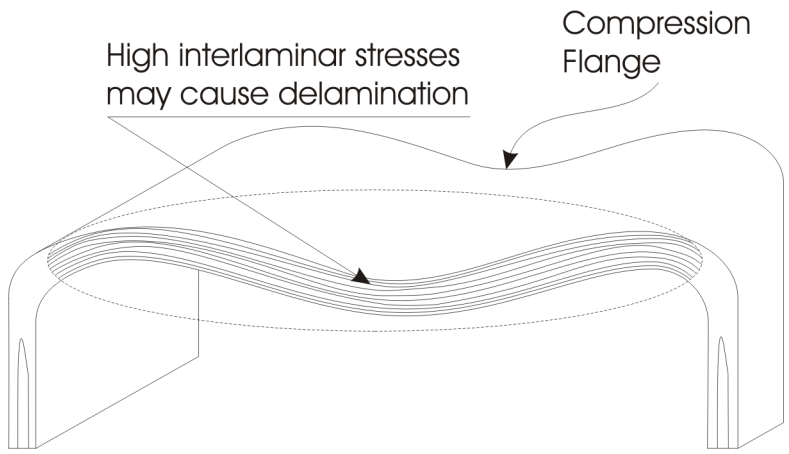

Figure 16. Transverse section of compression flange after snap-through

A FEM-simulation of the behaviour of a delaminated plate is exceedingly complexed. Partly because of this complexity, and partly because of the importance of the problem, this failure mode has received a great deal of attention recently. See review article by Yin (reference 19) and R. K. Kapania (reference 13).

In the litterature we have found many theories, which are developed to include delaminations, but none of these theories can be used in general cases and verified by experiments. Some researchers have developed different theories and implemented these in the FEM-calculations, but they all need extreme computation resources, so they cannot be used for practical purposes. See for example reference 20.

To describe the damage process of delaminated composites up to final failure three-dimensional Elasticity Models (reference 21) or Layerwise Plate Models (reference 22) are adequate to predict postbuckling behaviours of multiple delaminated composite laminates. However, this kind of analysis requires large amount of computer resources. Thus, for an engineering analysis to save computing time and memory, a “Global-Local Approach” is a suitable choice for compromising accuracy and efficiency. See reference 23. The “Global-Local Approach” use Layerwise Plate Elements in the local delaminated zone because

they actually describe the geometric deformations of the three-dimensional elements. In the undelaminated part, the first-order shear elements are used because the deformation patterns are less complicated than those of the delaminated zone.

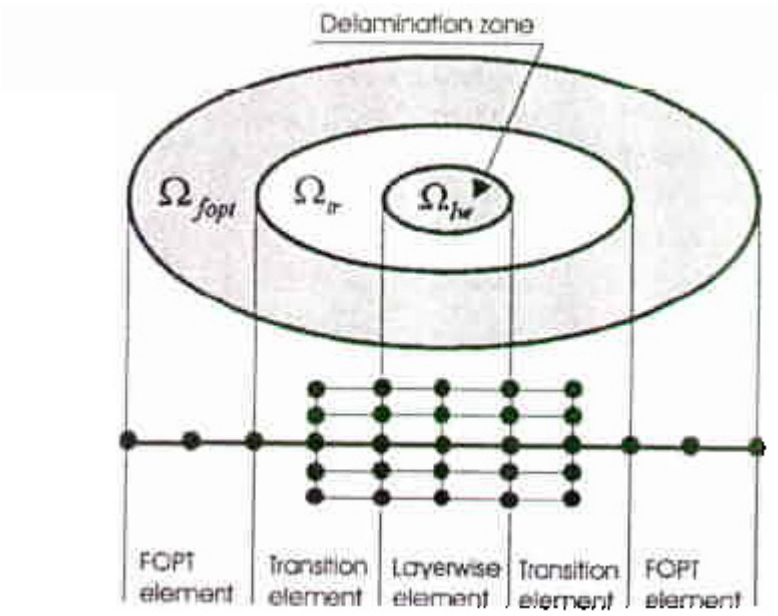

Figure 17. Definition of the transition domain, Reference 24

A transition element is developed in reference 24 to connect the global undelaminated zone and local delaminated zone.

Another theory that includes delaminations, is called “Higher-Order Zig-Zag Theory”. See reference 25. This theory decreased the computation resource dramatically and it included multiple delaminations, which is not implemented in the “Global-Local Approach”. The “Higher-Order Zig-Zag Theory” determines the number of degrees-of-freedom of an undelaminated zone independent of both the number of layers and the number of delaminations. In the delaminated zone, the minimal numbers degrees-of-freedom are still retained.

The theory used in the project is based on the Classic Laminate Theory (CLT) One of the limitations using Classic Laminate Theory, is that free edge effects are not included. Very high interlaminar stresses can arise at the free edge of a laminate with different ply orientations. This phenomenon has been studied extensively from the work of Pipes and Pagano reference 24 and Wisnom reference 26.

4.2.2 Kink Band Failure

Ply level fibre waviness may exist, which can be very important in compressive failure. See reference 2, 21 and 25. Resin rich regions, voids and delaminations can also be formed between plies. See references 22 and 26.

4.2.3 Matrix and Fibre Failure

Local micro cracks in the matrix and/or fibre matrix disbands were suggested, in references 26, as the most likely inherent flaws responsible for the decrease

in strength. A composite has defects as a result of its microstructure in addition to the flaws in the fibre and matrix. For example there are heterogeneties in the packing of the fibres which may give rise to local weakness: Clusters of closely packed fibres, resin rich regions, fibres debonded from the matrix, voids, broken or misaligned fibre. See reference 10, 26 and 27.

4.3 Description of modelling of structures with damages (e.g. delamination)

Concerning modelling of laminate failure, it is common to make a distinction between *initiation* and *progression*. Failure criteria for damage initiation are usually stress or strain based, i.e., damage or crack initiation is assumed to happen when a stress component or combination of stress components reach a critical value (See reference 30). Such criteria are easy to use in finite element models.

Once a crack has initiated, the next concern is to determine the conditions under which it propagates. This requires fracture mechanics modelling. The simplest fracture mechanics approach is linear elastic fracture mechanics (LEFM), in which linear elastic materials properties are assumed everywhere except for a very small region near the crack tip, where the material fails (See references 36 and 28). Then, crack growth is assumed to happen when the crack tip *stress intensity factor*, K, (that scales the singular crack tip stress and displacement fields) reaches a critical value, K_c, called the *fracture toughness*. Alternatively, a crack growth criterion can be based on the *energy release rate*, G; crack growth occurs when the energy release rate reaches a critical value, G_c, denoted the *fracture energy*. Within LEFM, the two criteria are equivalent. A complication is that crack growth in weak planes (e.g. delamination and crack in adhesive joints) occurs in combination of mode I ("opening") and mode II ("sliding"), so that *mixed mode* crack growth criteria must be used (See reference 33).

Due to the high stress gradients near the crack tip, a fine mesh is required in the crack tip region in FEM models of e.g. structures with a delamination. Stress intensity factors can be obtained e.g. by matching the FEM crack tip displacement field to the analytical solution, by energy methods (See reference 28) or by the path independent J integral (See reference 38). A full 3D analysis is computational demanding (See reference 37); therefore 2D models are used if possible.

Approaches for determining the shape of a crack front are developed. One method is to adjust the crack front (moving the crack tip nodes, node by node) so that the crack growth criterion is just full filled along the entire crack front (See reference 34). Another approach is *cohesive zone modelling* (See reference 31). In cohesive zone modelling the failure process zone is modelled by a non-linear stress-opening relationship (the cohesive law). The cohesive zone can be modelled at the expected cracking plane. Then, as the load is applied incrementally, the crack front automatically propagates as a part of the FEM solution (See references 35 and 29).

Delamination and splitting are often accompanied by fibre bridging. The energy uptake in the bridging zone can be much higher than the crack tip fracture energy (See reference 39). However, this cannot be accounted for in LEFM mod-

els; instead the fibre bridging must be modelled by cohesive laws (See reference 32). Methods for measurement of mixed mode cohesive laws are under development (See reference 4).

5 Comparison of Full-scale Test and FEM-simulation

Comparison between full-scale test and FEM-analysis has shown different postbuckling behaviour. The FEM-simulation evaluated in chapter 3, showed a long stable postbuckling behaviour. The full-scale measurements have shown a linear behaviour nearly until break, see figure below.

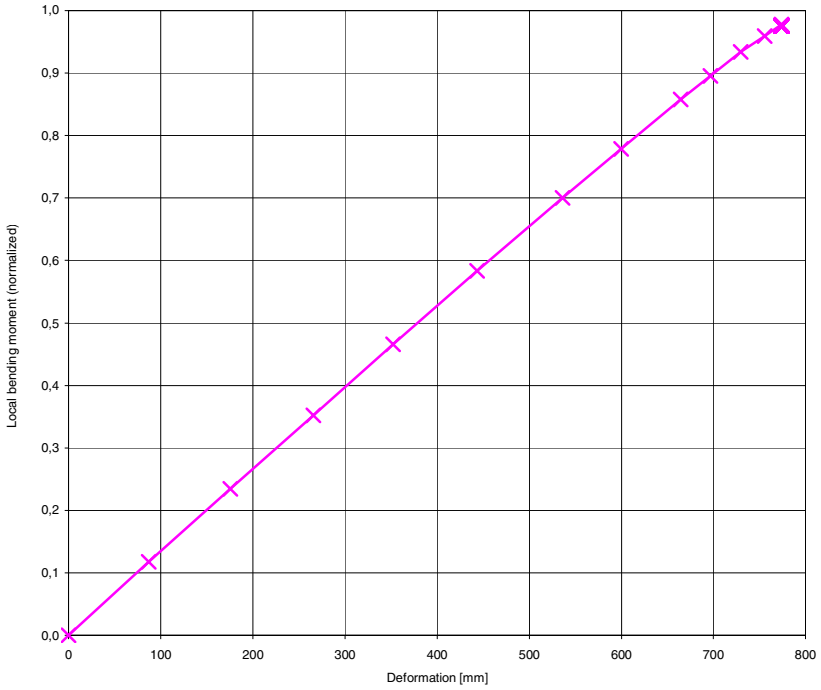

Figure 18: Load versus displacement curve recorded at the full-scale test (test section 3)

Unfortunately, it is not possible to compare slope and ultimate load, because of the difference in geometry, lay-up from the FEM-model and the full-scale test (Reference 3+5), see explanation page 6.

When we compare full-scale measurements figure 19 and FEM-simulations figure 12, the “relative deflections” in point A minus point B, show almost the same behaviour, which confirms that we actually have the bifurcation point just before the blade collapses.

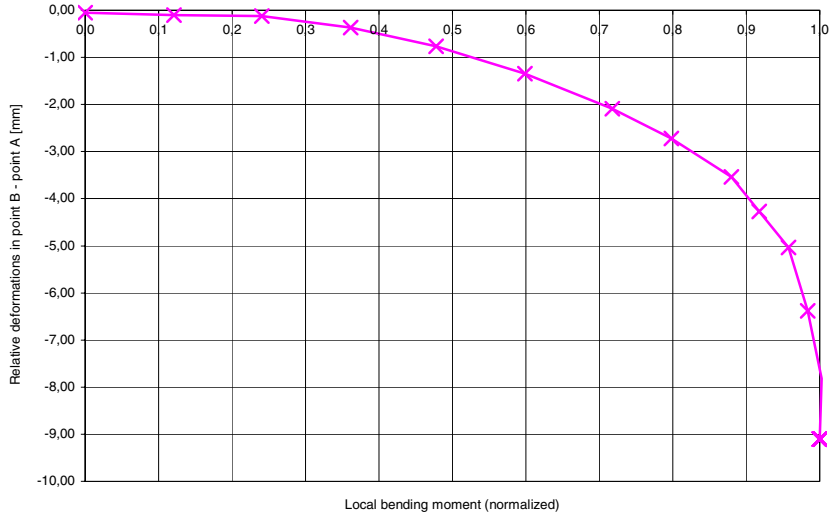

Figure 19: Displacement versus load recorded at the full-scale test (test section 3)

A comparison between the full-scale test (test 2) and the FEM-simulation has shown that the FEM-model predicts the ultimate buckling load to be approximately twice as high as the measured failure load. The "observation" is based on the difference from the measured strains when the main spar collapses and the calculated strains in the FEM-model. The calculated strains are based on the fact that the main spar does not collapse before the snap-through point is reached. If we instead evaluate the strains when we have the bifurcation load the deviation would have been much smaller.

This strain comparison is not very accurate, because the full-scale test creates collapse in the supports, see reference 3+5, so maybe the main spar could have obtained much more load if the collapse had happened another place.

6 Conclusion and Further Work

The main purpose with this first part of the project was to get an understanding of the buckling behaviour of a large blade structure and to find relevant failure mechanism, so relevant laboratory tests and FEM-simulations can be made in future work (phase 2).

6.1 Summary

Compressive stability FEM-simulations of composites are notoriously difficult, and despite the huge amount of research that has been undertaken there are still many problems to solve in the future.

In the FEM-simulation of the main spar, delaminations, imperfections, material degradation are not included. Therefore the result must be handled carefully. The full-scale experiment indicates that significant damage develops prior to failure.

The FEM-simulation of the load-displacement path, of the main spar, has shown a stable postbuckling behaviour after the bifurcation point. It can be concluded that strong orthotropic panel without delaminations, imperfection, material degradation and with a small curvature have a stable postbuckling behaviour. In case of no delaminations, the flanges will not be so sensitive to imperfections, but in cases where delaminations develop there will not be a long stable postbuckling behaviour and the load capacity will be sensitive to imperfections.

Unfortunately, it has not been possible to make real comparisons since the full-scale test of the modeled sections (test 2) broke in the supports. Full-scale of another section (test 3) was more successful, but we have not had the time in this first phase to update the FEM-model, this will be made in next phase.

In spite of the uncertainty it seems like the main spar collapses in the full-scale test a few seconds after the bifurcation limits are reached. A comparison between the full-scale test and FEM-simulation of the buckling behaviour of the compression flange and the load-deflection path has shown the same behaviour to the bifurcation point.

The FEM-model must be updated, to represent the geometry, lay-up, etc. in test 3 before more accurate and more exact conclusion can be made.

6.2 Further Work

A lot of improvement can be made in the FEM-simulation, but we believe that it is not realistic the next 3 – 5 years that FEM-models can be developed to give so accurate strength predictions that full-scale testing becomes unnecessary.

But in cases where advanced FEM-models are calibrated with experience from the laboratory and full-scale testing, we believe that it is possible to design the next generation of large blades without any major “surprises” in the final full-scale test. Today we find the FEM-tools, in this complicated area, very useful to improve the understanding of how composites in compression behave, and parameter analysis can show the tendency while changing some geometry or material parameters. Parameter analysis could investigate the buckling behaviour, when geometry, fibre lay-ups, material parameters etc. are changed.

6.2.1 Improvement of FEM-model of the Main Spar

- To have more accurate FEM-results, the geometry, lay-up, ply drops, etc. must be improved.
- Material degradations must be included, so the stiffness reduction in the lay-up is taken into account.
- Second order shear effects may improve the out of plane shear flexibility.
- Damage evolution (e.g. of delaminations) should be included.

6.2.2 Laboratory Tests and FEM-simulations in the future

In planning of future work, it must be considered whether laboratory tests should be made with “old” designs philosophy and old materials (glass fibre). Some blade manufacturers have already implemented carbon fibres in their new

blade designs. Carbon fibres, due to their high stiffness and low weight, a natural choice for future blade designs. However, carbon fibres are more sensitive for waviness and kink band failure, which maybe is one of the most important failure modes. In this case obtaining reliable and repeatable data for compressive strength is very important for the accuracy.

The failure analysis of delaminated plates is quite complicated because it includes postbuckling load increments, iterations of delamination zone propagation, and a contact algorithm between delaminated interfaces.

The effect of boundary conditions and other parameters (e.g., plate aspect ratio, imperfection sensitivity, thickness/radius ratio, etc.) may also be studied.

Laboratory test of a blade section, subjected to lateral load, verifying the rotationel stiffness could be one of the tests made in the next part (phase 2). See further explanation in reference 3. The results from the laboratory test, will be simulated with 2D-FEM-models which may included interlaminar failures (delaminations).

7 References

[1] Risø-R-1390(EN) "Fundamentals for improved design of large wind turbine blade of fibre composites based on studies of scale effects (Phase 1) - Summary Report" Bent F. Sørensen, AFM
ISBN 87-550-3176-5; ISBN 87-550-3177-3(Internet) ISSN 0106-2840

[2] Risø-R-1391(EN) "Indentification of Damage Types in Wind Turbine Blades Tested to Failure" Christian P. Debel, AFM
ISBN 87-550-3178-1; ISBN 87-550-3180-3(Internet) ISSN 0106-2840

[3] Risø-R-1392(EN) "Full scale testing of wind turbine blade to failure - flapwise loading" Erik Jørgensen, VEA
ISBN 87-550-3181-1; ISBN 87-550-3183-8(Internet) ISSN 0106-2840

[4] Risø-R-1394(EN) "A general mixed mode fracture mechanics test specimen for characterising adhesive joints" Bent F. Sørensen, AFM
ISBN 87-550-3186-2; ISBN 87-550-3187-0(Internet) ISSN 0106-2840

[5] Risø-I-1908(EN) "Full scale testing of wind turbine blade to failure - flapwise loading – test data - confidential" Christian Thomsen, SPK

[6] Arthur W. Leissa & Yoshihiro Narita. Recent Developments in Buckling Analysis of Laminated Composites Plates Ohio State University, USA & Hokkaido institute of Technology Composite structures 1992, pp. 629-635

[7] MSC Software Corporation, Version 2001
MSC.Marc Vol A: Theory and user Information
MSC.Marc Vol B: Element Library

[8] Hsuan-Teh Hu, Influence of In-Plane Shear Nonlinearity on Buckling and Postbuckling Responses of Composites Plates and Shells University Road Tainan, Taiwan Journal of Composites Materials, Vol. 27, Na2, 1993

[9] Allen, H. E. & Bulson, P. S.
Background to buckling
McGraw-Hill, London, 1980

[10] Pedersen P. Terndrup & Jensen, J. Juncher
Styrkeberegning af maritime konstruktioner, Del 3
Instituttet for skibs- og havteknik, DTH, 1983

[11] Bushnell, D.,Computerized buckling analysis of shells, 1985. Lockheed Palo Alto Research Laboratory, USA. Martinus Nijhoff Publishers

[12] Sheinmani & Simitses G.J., Buckling and Postbuckling of Imperfect Cylindrical Shells under Aksial Compression Composites Structures, Vol. 17 pp. 277

[13] Kapania R. K., A Review on the Analysis of Laminated Shells Virginia Polytechnic Institute and State University, Blacsburg, May 1989 Journal of Pressure Vessel Technology, Vol. III, pp. 88-96

[14] Zhangy & Matthews F.L.,Postbuckling of Cylindrical Curved Panels of Generally Layered Composites Materials with Small Initial Imperfections of Geometry, 1981. Composites Structures, Applied SciencePublisher, London pp. 428-441

[15] Jensen, H. M., "Three-dimensional numerical investigation of brittle bond fracture" International Journal of Fracture 114, 153-165, 2002.

[16] Budiansky, B. and Fleck, N. A. (1993) "compressive failure of fiber composites" Mech. Phys. Solids, Vol. 41, pp. 183-211

[17] Rieber, Hans Jørgen, Response Analysis of Dynamically Loaded Composite Panels Instituttet for skibs- og havteknik, DTU, 1997

[18] Reddy, J. N., "A generalization of Two Dimensional Theories of Laminated Composites Plates" Communications in Applied Numerical Methods, Vol. 3, No. 3, 1987, pp. 173-180

[19] Yin, W.-L., "Recent Analytical Results on Delamination Buckling and Growth" Interlaminar Fracture in Composite, A.E. Armanios, Ed., Trans. Tech. Publications, Ltd., Switzerland, 1989

[20] Whitcomb, J. D. Finite Element Analysis of Instability Related Delamination Growth Journal of Composites Materials, Vol. 15, Sept. 1981 pp. 403-426

[21] Maenghyo Cho & Jun-Sik Kim., Higher-Order Zig-Zag Theory for Laminated Composites With Multiple Delaminations, Inha University & Seoul University, Korea, Journal of Applied Mechanics, Vol. 68, November 2001, pp. 869-877

[22] WU L. C. & Kushner A., Identifying failure mechanisme of composites structures under compressive load, State University of New York Pergamon, PII: S0020-7683(97)00096-6, Int. J, Solids Structures, Vol. 35, No. 12, pp. 1137-1161, 1998

[23] Maenghyo Cho & Jun-Sik Kim, Bifurcation Buckling Analysis of Delaminated Composites Using Global-Local Approach, Inha University Korea AIAA Journal, Vol. 37, no 6: Technical notes, 2000, pp. 1673-1676

[24] Pipes R.B. & Pagano N., Interlaminare stresses in composites laminates under uniform axial tension, J. Compos Mater 1970; 4:538-48

[25] Jun-Sik Kim & Maenghyo Cho, Postbuckling of Delaminated Composites Under Compressive Loads Using Global-Local Approach, Inha University Korea AIAA Journal, Vol. 37, no 6: Technical notes, 2000, pp. 774-778

[26] Wisnom M. R., Size effects in the testing of fiber-composites materials, University of Bristol, Elsevier April 1999, Composites Science and Technology 59, 1937, pp. 1937-1957

[27] Kim K. & Voyiadjis G. Z., Buckling strength prediction of CFRP cylindrical panels using Finite Element Method, Composites Part A 30 1093-1104, Elsevier,1999

[28] Broek, D., 1986, Elementary engineering fracture mechanics, 4th edition, Mertinus Nijhoff Publishers, Dordrecht and Boston.

[29] Hansen, P. F., and Jensen, H. M., 2003."2-D cohesive zone modelling of interface fracture near flaws in adhesive bonds". In preparation.

[30] Hashin, Z., 1980, "Failure criteria for unidirectional fiber composites", Journal of Applied Mechanics, Vol. 47, pp. 329-34.

[31] Hutchinson, J. W, and Evans, A. G., 2000, "Mechanics of materials: Top-down approaches to fracture", Acta materialia, Vol. 48, pp. 125-35.

[32] Jacobsen, T. K., and Sørensen, B. F., 2001, "Mode I Intra-laminar crack growth in composites - modelling of R-curves from measured bridging laws", Composites part A, Vol. 32, pp 1-11.

[33] Jensen, H. M., 1990, "Mixed mode interface fracture criteria", Acta Metall. Mater., Vol. 38, pp. 2637-44.

[34] Jensen, H. M., Hutchinson, J. W., and Kim, K.-S., 1990, Decohesion of a cut prestressed film on a substrate", Int. J. Solid Structures, Vol. 26, pp. 1099-1114.

[35] Kafkalidis, M. S. and Thouless, M. D., 2002, "The effect of geometry and material properties of the fracture of single lap-shear joints", Int. J. Solids Structures, Vol. 39, pp. 4367-83.

[36] Kanninen, M. F., and Popelar, C. H., 1985, Advanced fracture mechanics, Oxford University Press, New York, p. 159.

[37] Nakamura, T., and Kamath, S. M., 1992, "Three dimensional effects in thin film fracture mechanics", Mechanics of Materials, Vol. 13, pp. 67-77.

[38] Rice, J. R., 1968, "A path independent integral and the approximate analysis of strain concentrations by notches and cracks", J. Appl. Mech., Vol. 35, pp. 379-86.

[39] Sørensen, B. F. and Jacobsen, T. K., 1998, "Large scale bridging in composites: R-curve and bridging laws", Composites part A, vol. 29A, pp. 1443-51.

8 Word explanations

Acoustic Emission (AE): A technique for detecting damage development in structure. Sensors detect stress waves emitted from an entity (e.g. a fibre) that fails

Bifurcation Buckling – The deformations begin to grow in a new pattern which is quite different from the prebuckling pattern

CLT - Classic Laminate Theory

Composite Material: A material consisting of two or more distinctive materials, such as fibres embedded in a continuous matrix. Example: Glass-fibre polyester

Damage: Non-catastrophic fracture events that develops in materials during mechanical loading

Debonding: A failure mode, where crack growth takes place along an interface between two dissimilar materials, e.g. in an adhesive joint or (at the microscale) between fibre and matrix

Defect: An undesired flaw or unwanted microstructural event, that are made during processing. Examples: Voids, un-wetted fibres in a material, pores in an adhesive joint

Delamination: Crack growth in the interface between (identical) plies in a laminated structure

FEM - Finite Element Method

Fibre composite: A composite material consisting of fibres embedded in a continuous matrix

Fibre kinking – A failure mode in fibre composites in compression. Failure occurs as
fibres buckles (microbuckling) due to compressive stresses and forms a band where fibres break (kink band)

Fibre waviness – A microstructural defect in laminates; when fibres are not straight

Fracture mechanics: A branch of solid mechanics, where strength of materials or structures are analysed on the basis of the presence of cracks

Lamina: A layer of (ortothropic) material, e.g. a layer of unidirectional fibre composite material

Laminate: A structure (plate/shell) consisting of layers of identical plies (laminas)

Main Spar - Box beam in a wing turbine blade structure

Matrix - The continuous phase in a composite material

MSC – MSC Software Corporation www.mscsoftware.com

NDT: Non Destructive Testing

Ply - A layer of composite material; often unidirectional or woven.

Resin – Adhesive used as matrix material in fibre composites

Snap Through Buckling - Loss of stability in plate

Wrinkling: A failure mode, where the face of a sandwich panel, buckles

Bibliographic Data Sheet **Risø-R-1393(EN)**

Title and authors

Compression Strength of a Fibre Composite Main Spar in a Wind Turbine Blade

Find Mølholt Jensen

ISBN	ISSN
87-550-3184-6 87-550-3185-4 (Internet)	0106-2840

Department or group	Date
Wind Energy Department	June 2003

Groups own reg. number(s)	Project/contract No(s)

Sponsorship

Pages	Tables	Illustrations	References
33		19	39

Abstract (max. 2000 characters)

In this report the strength of a wind turbine blade is found and compared with a full-scale test, made in the same project. Especially the postbuckling behaviour of the compression flange is studied. Different compressive failure mechanisms are discussed and the limitations in using the Finite Element Method. A suggestion to the further work is made.

Descriptors INIS/EDB